Molecular Crystals and Liquid Crystals Science and Technology. Section A. Molecular Crystals and Liquid Crystals
Publication details, including instructions for authors and subscription information:
http://www.tandfonline.com/loi/gmcl19

Non Isomorphism and Miscibility in The Solid State: Determination of The Equilibrium Phase Diagram n-Octadecane $C_{18}H_{38}$ + n-Nonadecane $C_{19}H_{40}$

L. Robles [a] , D. Mondieig [a] , Y. Haget [a] , M. A. Cuevas-diarte [b] & X. Alcobe [c]

[a] Laboratoire de Cristallographie et Physique Cristalline, CNRS-Université de Bordeaux I, 351, Cours de la Libération, F-33405, Talence

[b] Dept. Cristal. lografia, Mineralogia i Diposits Minerals, Fac. Geologia, Universitat de Barcelona, c/Marti i Franquès, E-08028, Barcelona

[c] Serveis Cientifico-Tecnics, Universitat de Barcelona, Lluis Solé i Sabaris 1-3, E-08028, Barcelona

Version of record first published: 04 Oct 2006.

To cite this article: L. Robles , D. Mondieig , Y. Haget , M. A. Cuevas-diarte & X. Alcobe (1996): Non Isomorphism and Miscibility in The Solid State: Determination of The Equilibrium Phase Diagram n-Octadecane $C_{18}H_{38}$ + n-Nonadecane $C_{19}H_{40}$, Molecular Crystals and Liquid Crystals Science and Technology. Section A. Molecular Crystals and Liquid Crystals, 281:1, 279-290

To link to this article: http://dx.doi.org/10.1080/10587259608042251

Mol. Cryst. Liq. Cryst., 1996, Vol. 281, pp. 279–290
Reprints available directly from the publisher
Photocopying permitted by license only

Non Isomorphism and Miscibility in The Solid State: Determination of The Equilibrium Phase Diagram n-Octadecane $C_{18}H_{38}$ + n-Nonadecane $C_{19}H_{40}$

L. ROBLES, D. MONDIEIG and Y. HAGET

Laboratoire de Cristallographie et Physique Cristalline, CNRS-Université de Bordeaux I, 351, Cours de la Libération, F-33405 Talence

M. A. CUEVAS-DIARTE

Dept. Cristal.lografia, Mineralogia i Diposits Minerals, Fac. Geologia, Universitat de Barcelona, c/Marti i Franquès, E-08028 Barcelona

X. ALCOBE

Serveis Cientifico-Tecnics, Universitat de Barcelona, Lluis Solé i Sabaris 1-3, E-08028 Barcelona

(Received October 30, 1995; in final form November 17, 1995)

The phase diagram of the binary n-alkane system $C_{18}H_{38}$–$C_{19}H_{40}$ is determined by calorimetric and X-ray diffraction methods. The present experimental results and previous work on pure $C_{18}H_{38}$ and $C_{19}H_{40}$ paraffins allow us to identify all the phases of the binary system. The phase diagram exhibits no less than six distinct solid domains: three are one-phase regions, triclinic (T), orthorhombic (O) and face-centered orthorhombic, called rotator phase (RI), and three are two-phase equilibria [T + O], [T + RI] and [O + RI]. The two regions [O] and [RI] occur on large composition ranges (from the pure constituent $C_{19}H_{40}$). The solid-liquid equilibria are separated by a eutectic invariant. They can be explained in terms of crossed isodimorphism.

Keywords: n-Octadecane, n-nonadecane, phase diagram, mixed crystal, rotator phase, crossed isodimorphism.

1. INTRODUCTION

The work presented here on the system $C_{18}H_{38}$–$C_{19}H_{40}$ is part of a general study concerning the syncrystallization of substances in the alkane family. This family was chosen for two reasons: to investigate the incidence of polymorphism of pure components on the formation of molecular mixed crystals, but also to study the possibilities to get molecular alloys with a strong energetic melting for thermal energy storage.

The non-isomorphism of the components, both at low and high temperature, implies two segregation domains. They were not established in the previous determination of this system, performed by Boutch, Alexandrova and Kiprianova (1984)[1]. Our purpose is to learn how important, the domains of stability of the molecular alloys and the domains of demixing are.

2. EXPERIMENTAL PART

2.1 Materials

The compounds $C_{18}H_{38}$ and $C_{19}H_{40}$ were purchased from Fluka with purity grades certified > 99%. These grades determined by gas chromatography and mass spectral analysis are more exactly 99.4% for $C_{18}H_{38}$ and 99.3% for $C_{19}H_{40}^{(*)}$ (percentage by weight). At these percentages, the impurities do not affect the phase behaviour to any significant extent.

Binary mixtures were prepared according to the "melting-quenching" method: the solid components are weighted in the desired molar fractions; the whole is heated up to the melting and mixed to get an entirely homogeneous sample which is then quenched into liquid nitrogen; it is kept at 278 K.

2.2 X-ray Powder Diffraction Analysis

Diffraction patterns were performed using a Siemens D500 vertical powder diffractometer which works in the reflection mode with CuK_α radiation ($\lambda = 1.5418$ Å) and with a curved graphite monochromator in the diffracted beam. This instrument uses a scintillation counter with a digital registration. The temperature was controlled with a low temperature Anton Paar TTK device, the stability being 0.1 K. The data were collected with 0.025° 2θ steps and 4 s interval time.

The samples were kept at constant temperature during the X-ray diffraction measurements. The analyses were made at increasing temperature, with 1 K step, especially in the composition regions near to the two phase domains.

2.3 Calorimetric Measurements

The calorimetric measurements were made with a Perkin-Elmer DSC7 calorimeter with its nitrogen sub-ambient accessories. The instrument was calibrated with the use of the known transition temperatures and enthalpies of indium, naphthalene and water standards.

Samples in sealed aluminium pans were heated from 253 K to beyond the liquidus temperature. Transition temperatures and enthalpies were determined from six independent experiments carried out on 4 mg samples, with 2 $K.min^{-1}$ speed of heating. The analysis method of the DSC curves is described elsewhere.[2,3] The random part of the uncertainties is estimated using the Student's method, with a 95% threshold of reliability; systematic errors are taken to be ± 0.5 K and $\pm 7\%$ $J.mol^{-1}$.

3. PURE COMPONENTS

3.1 n-octadecane [$C_{18}H_{38}$]

The crystal structure of the low temperature phase of C_{18} was earlier determined as triclinic corresponding to the space group $P\bar{1}$ with $Z = 1$,[4] (hereafter referred to as T phase).

* From now, we will use the abbreviations C_{18} for $C_{18}H_{38}$ and C_{19} for $C_{19}H_{40}$.

Our study by X-ray powder diffraction at 291 K gave lattice parameters:

$a = (4.334 \pm 0.008)$ Å $\quad b = (4.843 \pm 0.010)$ Å $\quad c = (25.09 \pm 0.07)$ Å
$\alpha = (84.97 \pm 0.07)°$ $\quad \beta = (67.3 \pm 0.2)°$ $\quad \gamma = (72.56 \pm 0.10)°$

These values are near those of the literature.[5,6,7]

The phase T remains until the melting point at (301.1 ± 0.6) K. The enthalpy variation for the phase T to liquid is (59.8 ± 4.1) kJ.mol^{-1}. These energetic results are in good agreement with those of previous publications.[8,9]

3.2 n-nonadecane [$C_{19}H_{40}$]

It has been shown that below 294 K, the crystal structure is orthorhombic (Pbcm, $Z = 4$).[10] Hereafter, we refer this phase as O. The parameters obtained by X-ray powder analysis are at $T = 291$ K:

$a = (4.989 \pm 0.005)$ Å $\quad b = (7.482 \pm 0.010)$ Å $\quad c = (51.96 \pm 0.08)$ Å

These values are in agreement with the literature.[11,12]

At increasing temperature, after 294 K, the structure becomes face-centered orthorhombic (Fmmm, $Z = 4$).[13] This phase presents a rotational disorder and is commonly called rotator phase (RI). X-ray powder patterns of this phase present few diffraction lines, usually we observe 004, 006, 008, 111 and 020 in the 2θ range studied (2θmax. = 40°) with considerable background scattering (a characteristic phenomenon of this phase). The particularity of RI is the evolution of parameters (a and b) as a function of the temperature, see Table I. The b/a ratio tends to of $\sqrt{3}$ without reaching it. The temperature and enthalpy variation of O to RI phase transition are, respectively, (294.8 ± 0.6) K and (12.7 ± 0.5) kJ.mol^{-1}. The corresponding values for melting are (304.4 ± 0.7) K and (42.7 ± 3.2) kJ.mol^{-1}. As for C_{18}, these values are in good agreement with those of the literature.[8,9]

4. DETERMINATION OF THE EQUILIBRIUM PHASE DIAGRAM

4.1 Limits of the Syncrystallization Domains

The X-ray experiments have been performed on nineteen binary mixtures. Their qualitative results are presented in Figure 1. This analysis informs us of the behaviour of the equilibrium diagram in the solid state. Three solid phases are identified O, RI and

TABLE I
Temperature Influence on the Parameters a and b of the RI phase of $C_{19}H_{40}$

T in K	a(Å)	b(Å)	c(Å)	b/a	Reference
296	5.10	7.63	52.32	1.50	11
296	5.07	7.70	52.3	1.52	This work
299	5.06	7.74	52.3	1.53	This work
303	5.03	7.87	52.4	1.57	This work

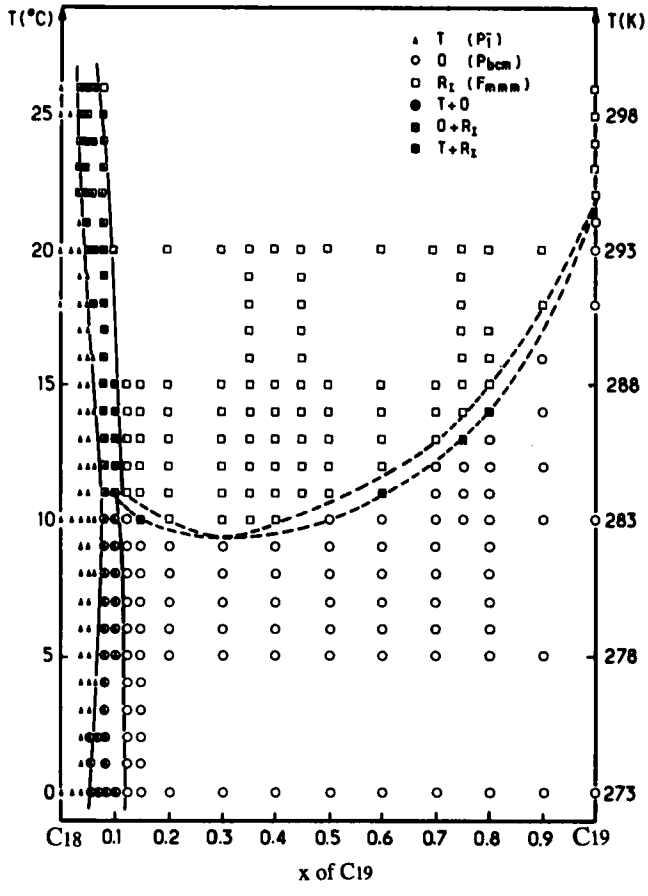

FIGURE 1 X-ray measurements as a function of molar concentration and of temperature at the solid state. (▲) domain of mixed crystal with triclinic (T) structure. (○) and (□) domains of molecular alloys with orthorhombic (○) structure and face centred orthorhombic (RI) structure respectively. (⊡), (●) and (■) biphasic domains [O + RI], [T + O], and [T + RI] respectively.

T. The two phase regions [T + O] and [T + RI] are delimited. From X-ray diffraction measurements, they are clearly distinguished by the coexistence of two typical patterns. The two biphasic domains are very narrow; they are observed for the samples with molar fractions of C_{19} ranging between 0.04 and 0.11. Hence it follows that the two regions [O] at low temperature and [RI] below the melting temperature, respectively, exist in very large ranges of compositions.

Figures 2 and 3, which represent the long spacing evolution ($d_{00\ell}$) as function of composition at 273 K and 293 K respectively, quantitatively illustrate these behaviours. At 273 K, the molecular alloy region with triclinic structure T is very narrow, its limits are pure component C_{18} to $(C_{18})_{0.96}$ $(C_{19})_{0.04}$, whereas for the orthorhombic structure O they range from $(C_{18})_{0.89}(C_{19})_{0.11}$ to pure C_{19}. At 293 K, the [T] domain is nearly the same as at 273 K, while the [RI] one enlarges from $(C_{18})_{0.92}(C_{19})_{0.08}$ to $(C_{18})_{0.05}(C_{19})_{0.95}$.

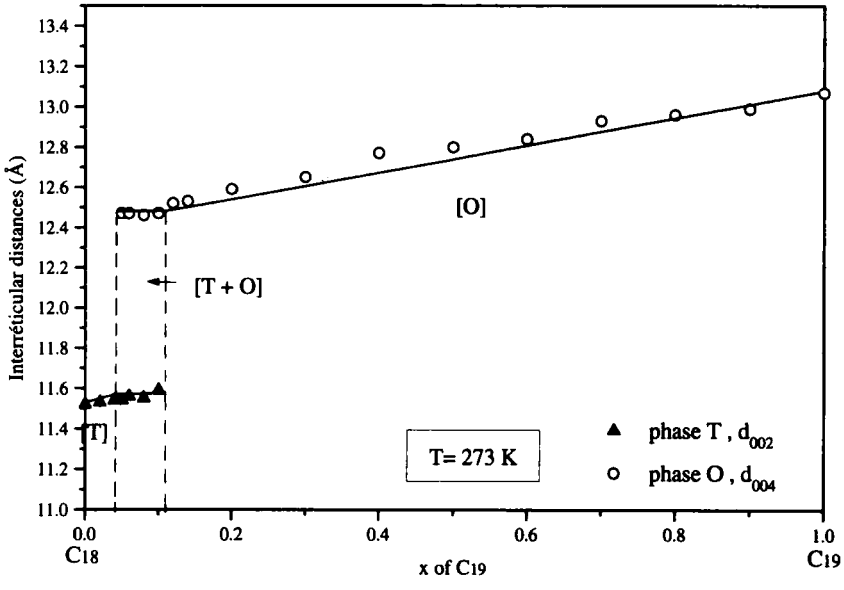

FIGURE 2 Long spacing $d_{00\ell}$ evolution as a function of molar composition at $T = 273$ K. (▲) d_{002} of triclinic phase, (○) d_{004} of orthorhombic phase.

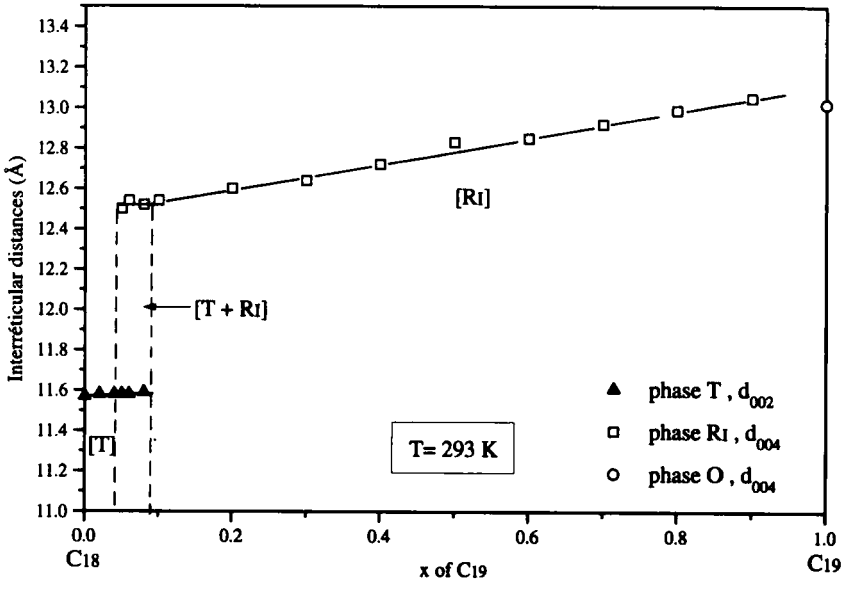

FIGURE 3 Long spacing $d_{00\ell}$ evolution as a function of molar composition at $T = 293$ K. (▲) d_{002} of triclinic phase, (□) d_{004} of RI phase.

Powder diffraction patterns at different temperatures point out the existence of the peritectoid invariant (for the molar fraction $x = 0.10$ of C_{19}), they are given in Figure 4. This invariant separates the two [T + O] and [T + RI] biphasic domains at increasing temperature. Its crossing is observed by the reflection continuity of the triclinic phase and the vanishing of two characteristic $(1\bar{1}0)_O$ and $(020)_O$ reflections from phase O, with the concomitant appearance of two reflections $(111)_{RI}$ and $(020)_{RI}$ of phase RI.

The X-ray and calorimetric experiments allow us to characterize this invariant: the left and right limits are the molar fraction $x = 0.07$ and $x = 0.13$ of C_{19}, and the peritectoid composition is $x = 0.10$ of C_{19} at $T_p = (283.9 \pm 0.6)$K.

4.2 The [O + RI] domain

Figure 5 illustrates the typical DSC curves obtained for each composition of this alkane system. From $x = 0.13$ to pure component C_{19}, the weaker peak corresponds to the $O \rightarrow RI$ phase change. The analysis of this part of measured curves shows the presence of a Gibbs minimum point, near the molar fraction $x = 0.30$ of C_{19}.

The energetic parameters of this transition (inferior and superior solvus temperatures and enthalpies of transition) are reported in Table II. This two-phase region is very narrow, less than 1 K. The enthalpies involved in this phase change are about 7000 $J.mol^{-1}$, which are high, but still much less than those of melting.

4.3 The solid-liquid equilibria

From calorimetric measurements, the peak analysis for the melting of all compositions leads us to propose two [T + L] and [RI + L] domains of equilibrium with a eutectic

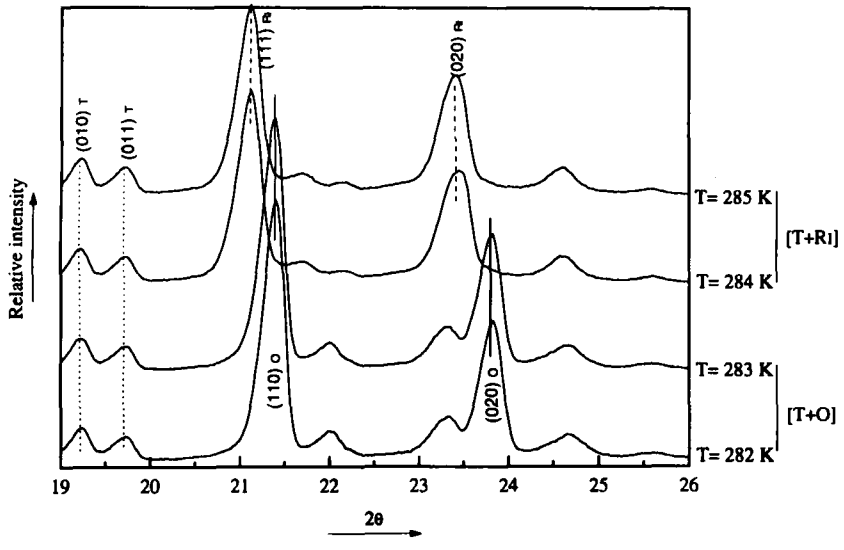

FIGURE 4 Existence of the peritectoid invariant (molar fraction $x = 0.10$ of C_{19}).

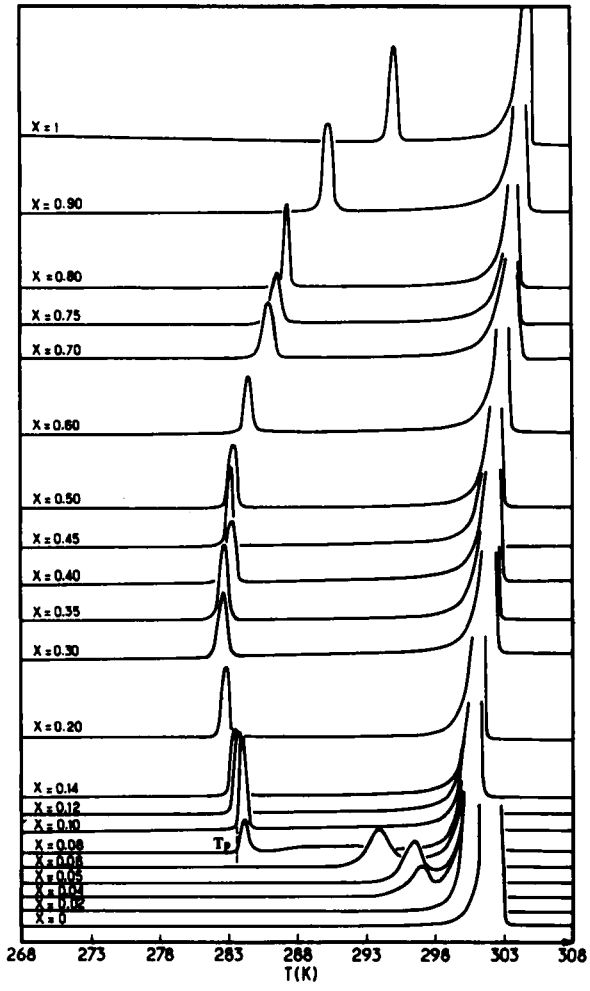

FIGURE 5 Evolution of DSC curves as a function of molar fraction (x of C_{19}) and temperature.

invariant for the compositions near the constituent C_{18}. Again the [RI + L] loop is very narrow in temperature (about 1 K) and covers the largest range of compositions. The limits of the eutectic invariant are the molar fractions $x = 0.03$ and $x = 0.06$ of C_{19}. The eutectic point is near the molar fraction $x = 0.07$ of C_{19} at $T_E = (299.9 \pm 0.6)$ K.

Energetic parameters of melting are reported in Table III with solidus, liquidus and eutectic temperatures and corresponding melting enthalpies. These last ones are high: about 60 kJ·mol^{-1} for the triclinic molecular alloys, and about 40 kJ.mol^{-1} for the RI mixed crystals.

5. DISCUSSION

The calorimetric and X-ray systematic studies of the binary mixture $C_{18}H_{38}$–$C_{19}H_{40}$ permit us to conclude that the final phase diagram presented in Figure 6 is character-

TABLE II
Temperature and Enthalpy Parameters of the O → RI Solid Transition for the C_{18}–C_{19} System Versus the Molar Fraction x of C_{19}

x	*Ti.solv* (*K*)	*Tp* (*K*)	*Ts.solv* (*K*)	ΔHtr(O → RI) ($kJ.mol^{-1}$)
0.08	–	283.8 ± 0.7	–	–
0.10	–	283.8 ± 0.7	–	–
0.12	283.5 ± 0.7	284.1 ± 0.7	–	–
0.14	283.2 ± 0.6	283.7 ± 0.6	–	7.4 ± 0.3
0.20	282.6 ± 0.6	–	283.3 ± 0.6	7.2 ± 0.3
0.30	282.5 ± 0.5	–	283.0 ± 0.7	7.0 ± 0.2
0.35	282.5 ± 0.5	–	283.0 ± 0.6	7.1 ± 0.3
0.40	282.9 ± 0.5	–	283.5 ± 0.7	7.1 ± 0.3
0.45	283.2 ± 0.6	–	283.5 ± 0.7	7.1 ± 0.3
0.50	283.2 ± 0.6	–	283.8 ± 0.6	7.1 ± 0.3
0.60	284.5 ± 0.6	–	284.9 ± 0.7	7.1 ± 0.2
0.70	285.6 ± 0.6	–	286.4 ± 0.7	7.5 ± 0.3
0.75	286.4 ± 0.6	–	287.0 ± 0.6	7.4 ± 0.3
0.80	287.3 ± 0.6	–	287.7 ± 0.7	7.4 ± 0.3
0.90	290.1 ± 0.6	–	290.9 ± 0.7	9.6 ± 0.4
1	294.8 ± 0.6	–	–	12.7 ± 0.5

TABLE III
Temperature and Enthalpy Parameters of melting for the C_{18}–C_{19} System Versus the Molar Fraction x of C_{19}

x	*Tsol* (*K*)	*TE* (*K*)	*Tliq* (*K*)	ΔHf ($kJ.mol^{-1}$)
0	301.5 ± 0.6	–	–	59.8 ± 4.1
0.02	300.1 ± 0.6	–	300.7 ± 0.7	58.9 ± 4.1
0.04	–	299.9 ± 0.6	300.2 ± 0.6	38.8 ± 3.8
0.05	–	300.0 ± 0.6	300.4 ± 0.6	38.5 ± 3.8
0.06	–	299.9 ± 0.6	300.2 ± 0.7	38.3 ± 3.8
0.08	300.1 ± 0.7	–	300.5 ± 0.7	39.5 ± 3.0
0.10	300.2 ± 0.7	–	300.6 ± 0.6	39.9 ± 3.0
0.12	300.2 ± 0.7	–	300.7 ± 0.7	40.3 ± 3.1
0.14	300.3 ± 0.7	–	300.7 ± 0.7	40.9 ± 3.1
0.20	300.6 ± 0.7	–	301.1 ± 0.7	40.4 ± 2.8
0.30	300.9 ± 0.8	–	301.5 ± 0.7	40.5 ± 2.8
0.35	300.9 ± 0.7	–	301.7 ± 0.7	40.6 ± 3.1
0.40	301.4 ± 0.7	–	302.0 ± 0.6	40.8 ± 3.4
0.45	301.6 ± 0.7	–	302.0 ± 0.7	41.2 ± 3.2
0.50	301.9 ± 0.6	–	302.3 ± 0.6	41.0 ± 3.2
0.60	302.5 ± 0.7	–	302.9 ± 0.6	41.0 ± 3.1
0.70	302.9 ± 0.6	–	303.5 ± 0.7	43.6 ± 3.2
0.75	303.1 ± 0.7	–	303.6 ± 0.7	41.9 ± 3.2
0.80	303.3 ± 0.6	–	303.8 ± 0.7	40.7 ± 3.1
0.90	304.0 ± 0.5	–	304.4 ± 0.7	41.9 ± 3.0
1	304.5 ± 0.7	–	–	42.7 ± 3.2

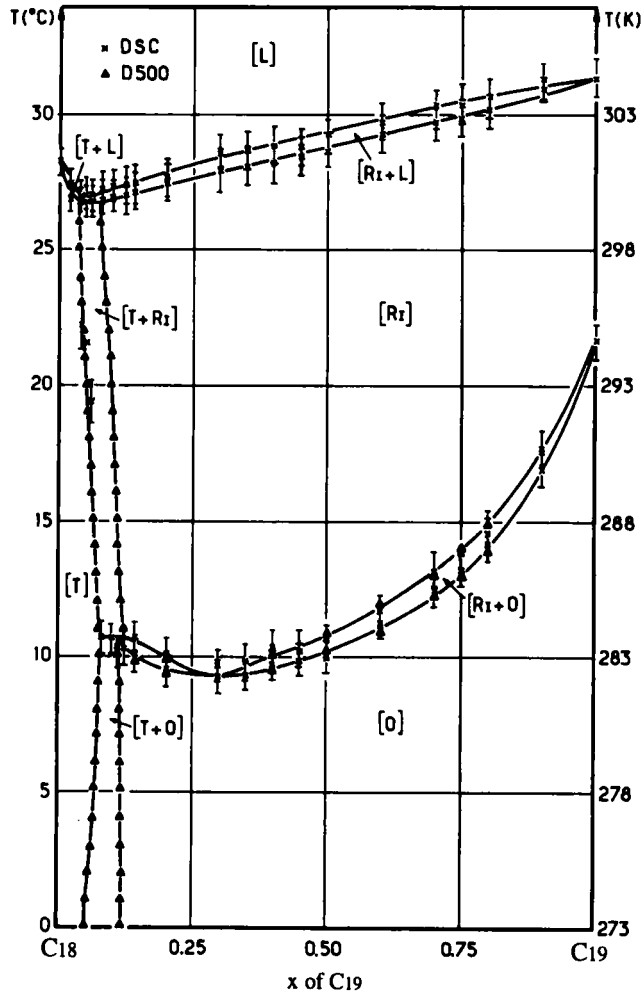

FIGURE 6 Phase diagram of the binary system: $C_{18}H_{38}$–$C_{19}H_{40}$.

ized by:

- the existence of the following regions:

(i) three stable solid solution domains with alloys of type T with a large range of x, alloys of type O at low temperature on a very large range of compositions; alloys of type RI, stable at high temperature on a range of compositions comparable to the previous one.
(ii) three solid-solid regions [T + O], [T + RI] and [O + RI],
(iii) two solid-liquid [T + L] and [RI + L] equilibrium domains.

- the existence of both a peritectoid and a eutectic invariants; their widths are very weak and both are in the vicinity of pure C_{18}.

The low temperature phase O and the rotator phase RI before melting are the most extended phases. From a structural point of view, at a given (constant) temperature the two types of alloys have nearly the same behaviour concerning their cell parameter variations versus the molar fraction x:

- in terms of a and b parameters their packing is quasi-constant whatever is x e.g.:

$$\text{at } 273\,\text{K}, \quad a_{\text{O}}(x) \cong 5.00\,\text{Å}; \; b_{\text{O}}(x) \cong 7.48\,\text{Å}$$

$$\text{at } 293\,\text{K}, \quad a_{\text{RI}}(x) \cong 5.05\,\text{Å}; \; b_{\text{RI}}(x) \cong 7.70\,\text{Å}$$

- the molecules being extended along the c axis, this parameter is of course strongly dependent on the molar fraction and increases continuously with x (see Figs. 2 and 3).

On the contrary, the dependence of the stacking versus temperature is quite different for the two types of alloys. The O alloys are very low dependent on temperature whereas the RI alloys which show a rotational disorder of the molecules along their c long axis, are very affected by the temperature. Their disorder strongly increases with temperature; this fact is reflected by a_{RI} and b_{RI} temperature dependence. The $b_{\text{RI}}/a_{\text{RI}}$ ratio tends to the value of $\sqrt{3}$ without reaching it. This value is only reached for longer n-alkanes[14] ($22 \leqslant n \leqslant 26$) to give a hexagonal stacking.

The obtained phase diagram with only partial miscibilities is in agreement with the non-isomorphism of pure components. However, the solid-liquid equilibria can be interpreted in terms of crossed isodimorphism,[15, 16] i.e. they can be considered as the result of the intersection of two solid-liquid loops [T + L] and [RI + L] each of them involving both a stable (s) and a metastable (m) phase. In fact, the experimental part of the [T + L] loop is too weak to attempt its extrapolation. On the other hand it is quite easy to do such an extrapolation for the experimental [RI + L] loop. It goes to the same $T_{(\text{RI}\rightarrow\text{L})\text{m}}$ for pure C_{18} as estimated by the study of the polymorphism of the C_nH_{2n+2} series with n going from 8 to 28[15, 17] ($T_{(\text{RI}\rightarrow\text{L})\text{m}} = 299.5\,\text{K}$). In the same way (extrapolation of the experimental values and analysis of polymorphism[15, 17]) it is possible to get the cell parameters of the metastable RI form of C_{18}. Due to the fact that the cell parameters are significantly temperature dependent, it is necessary to consider a normalized temperature T_{Ni} ($T_{\text{Ni}}/T_{\text{melting}} = \text{constant}$) to compare the two structural buildings (C_{18}(RI)m and C_{19}(RI)s). We adopt $T_{\text{Ni}}/T_{\text{melting}} = 0.995$;

$$\text{i.e.: } T_{\text{N}} = 298\,\text{K for } C_{18}$$

$$T_{\text{N}} = 303\,\text{K for } C_{19}$$

so that,

$$C_{18}\text{(RI)m} \quad 298\,\text{K} \quad a = 5.03\,\text{Å}, \quad b = 7.80\,\text{Å}, \quad c = 49.6\,\text{Å}$$

$$C_{19}\text{(RI)s} \quad 303\,\text{K} \quad a = 5.03\,\text{Å}, \quad b = 7.87\,\text{Å}, \quad c = 52.4\,\text{Å}$$

Now, it is possible to estimate the degree of crystalline isomorphism[18, 19] between the RI forms using ε_m^i which compare the two crystalline cells (m for "maille" in French).

The result is: $$\varepsilon_m^i(\mathrm{RI}) = 0,94.$$

This value, near 1, may be considered[15] as a very high value which is quite in agreement with the (very) large domain of RI syncrystallization.

A similar comparison may be made for the O type alloys at a lower temperature in introducing an O metastable form of C_{18}, the characteristics of which are:[15]

$$C_{18}(\mathrm{O})\mathrm{m}: \quad T_{(\mathrm{O}\rightarrow\mathrm{RI})\mathrm{m}} = 289.8\,\mathrm{K}$$

$$a = 5.00\,\text{Å}, \quad b = 7.46\,\text{Å}, \quad c = 49.6\,\text{Å}.$$

We get a degree of crystalline isomorphism:

$$\varepsilon_m^i(\mathrm{O}) = 0,95.$$

i.e a high value in agreement with the large domain of existence of form O.

On an other hand one has to note that all the enthalpies of melting of the various alloys are very important, the highest being that of the triclinic alloys. This property added to the fact that the thermal window[20] of melting is always very narrow (less than 1 K) enables us[20, 21] to say that these materials are good candidates to store or restore heat for storage applications.

Acknowledgments

This study has been partially supported by DGICYT (project number PB92-0800-C03-01).

References

1. L. J. Boutch, E. A. Alexandrova and E. N. Kiprianova, "Comptes rendus du centre scientifique Nord-Caucasien de l'école supérieure" pp 1–10 (1984).
2. R. Courchinoux, N. B. Chanh, Y. Haget, E. Tauler and M. A. Cuevas-Diarte, *Thermochimica Acta* **128**, 45 (1988).
3. R. Courchinoux, N. B. Chanh, Y. Haget, T. Calvet, E. Estop and M. A. Cuevas-Diarte, *J. Chim. Phys.* **86**(3), 56 (1989).
4. A. I. Kitaigorodsky, *Acta Cryst.*, **10**, 802 (1957).
5. A. Muller and K. Lonsdale, *Acta Cryst*, **1**, 129 (1948).
6. T. Hayahida, *J. Phys. Soc. Japan*, **17**, 306 (1962).
7. S. C. Nyburg and H. Luth, *Acta Cryst.*, **B28**, 2992 (1972).
8. A. A. Schaerer, C. J. Busso, A. E. Smith and L. B. Skinner, *J. Am. Chem. Soc.*, **77**, 2017 (1955).
9. P. Barbillon, L. Schuffenecker, J. Dellacherie, D. Balesdent and M. Dirand, *J. Chim. Phys.*, **88**, 91 (1991).
10. P. W. Teare, *Acta Cryst.*, **12**, 294 (1959).
11. R. D. Heyding, R. E. Russel, T. L. Varty and D. St-Cyr, *Powder Diffraction*, **5**, 2, 93 (1990).
12. A. R. Gerson, K. J. Roberts and J. N. Sherwood, *Acta Cryst.*, **B47**, 280 (1991).
13. G. Ungar, *J. Phys. Chem.*, **87**, 689 (1983).
14. L. Robles, D. Mondieig, Y. Haget, M. A. Cuevas-Diarte and X. Alcobe, *Les Equilibres entre Phases XX*, Ed. Haget and Marbeuf, 161 (1994).
15. L. Robles, *Thése de l'Université Bordeaux I*, (1995).

16. Y. Haget, H. A. J. Oonk and M. A. Cuevas-Diarte, *Les Equilibres entre Phases XVI*, Ed. Kaloustian and Pastor, Marseille, 35 (1990).
17. Y. Haget, D. Mondieig, P. Espeau, L. Robles, M. A. Cuevas Diarte and H. A. J. Oonk, *J. Chim. Phys.* (to be published).
18. Y. Haget, N. B. Chanh, A. Meresse and M. A. Cuevas-Diarte, *Phase Eq. Data Proceeding*, **1**, 170 (1985).
19. F. Michaud, *Thèse de l'Université Bordeaux* I, p 232 (1994).
20. Y. Haget, D. Mondieig and M. A. Cuevas-Diarte, Brevet CNRS FR91/08695.
21. M. Labrador, T. Calvet, M. A. Cuevas-Diarte, D. Mondieig, J. R. Housty and Y. Haget, *Mat. Res. Bull.*, **26**, 749–761 (1991).